Proceedings of IPC 2006
6th International Pipeline Conference
September 25-29, 2006, Calgary, Alberta, Canada

IPC2006-10487

PROBABILISTIC ASSESSMENT OF A 70-YEAR-OLD PIPELINE SUBJECT TO SEISMIC DEFORMATION

Robert W. Warke
LeTourneau University
Longview, Texas, USA

James D. Hart
SSD, Inc.
Reno, Nevada, USA

Ben H. Thacker
Southwest Research Institute
San Antonio, Texas, USA

ABSTRACT

This paper presents an assessment case study on several segments of buried natural gas pipeline constructed in 1936 with 'bell-bell-chill ring' (BBCR) style girth weld joints, and currently operating in a seismically active region of North America. Seismic vulnerability was evaluated in terms of girth weld fracture and plastic collapse probabilities for specified hazards of varying severity and likelihood. Monte Carlo simulations performed in NESSUS® provided failure probability estimates from distributed inputs based on PIPLIN deformation analyses, nondestructive and destructive flaw sizing, residual stress measurements, weld metal tensile and CTOD tests, and limit state functions based on published stress intensity and collapse solutions.

INTRODUCTION AND BACKGROUND

Over the past decade or so, a major owner/operator that chooses to remain unidentified has been engaged in an ongoing girth weld inspection and assessment program for a buried gas transmission pipeline of pre-World War II construction. Their previous work had been focused on developing critical flaw height *vs.* length curves as acceptance criteria for nondestructive inspection. These were initially developed for a series of assumed seismic loading magnitudes in various combinations with other sources of loading, but the criteria ultimately applied were simply based on an assumed maximum tensile stress of 30 ksi. Despite this and several other conservatisms that were adopted, fewer than 3% of the first ~250 arc-welded BBCR joints inspected were considered rejectable. Given these results, coupled with the high cost of girth weld inspection, the owner/operator entertained a proposal to reassess the pipeline on a probabilistic basis.

Segments of this pipeline in regions subject to large-scale ground failure (liquefaction, fault rupture, *etc.*) were already replaced or designated for such, and therefore outside the scope of this work. At the opposite end of the soil response spectrum were regions subject only to elastic shaking strains due to traveling waves, for which acceleration-strain relationships based on maximum ground particle and apparent shear wave propagation velocities have been established [1,2]. It is not overly conservative in the latter case to assume perfectly efficient soil-to-pipe strain transfer. Annualized probability density functions for pipeline strain can therefore be estimated directly from available peak ground acceleration (PGA) hazard curves. Compared to the uncertainty of event occurrence itself, the uncertainties of soil and pipe response due to elastic shaking alone are relatively small, and the likelihood of pipeline failure is negligible [3,4].

The present study was to address the 'middle ground' between these two extremes, where reasonably postulated seismic events could induce a limited but significant degree of permanent ground strain (landslide, lurching, *etc.*). Hazards of this kind were reportedly conceivable, if not probable, in regions comprising more than 90% of the pipeline's total length. Pipe-soil interaction was therefore a major contributor to the overall uncertainty of its seismic fitness. The present assessment addressed five separate segments of 'old' pipeline operating in such areas.

OBJECTIVES

The primary objectives of this study were to:

1. Define relevant failure criteria for BBCR girth welds in five segments of a pre-World War II vintage pipeline subject to various levels of deformation during potential seismic events.
2. Incorporate available BBCR girth weld properties data and the results of PIPLIN-based seismic deformation analyses into suitable probability density functions.
3. Compute the overall girth weld failure probability within each segment for the range of postulated seismic events represented by the deformation analyses.
4. Interpret the results to enable an informed fitness-for-service (FFS) decision by the owner/operator for each segment.

PROCEDURE AND RESULTS

The following sections describe the tasks undertaken and results obtained to achieve the stated objectives.

Defining Failure Criteria

As in a deterministic FFS assessment, a probabilistic assessment requires a mathematical description of the criterion by which each of

the potential failure modes is defined. For sake of convenience in probabilistic calculations, this is generally expressed as a limit state function of the form:

$$P_f = P\left[g(X_1, X_2, \ldots, X_n) \le 0\right] \tag{1}$$

where X_i are the random variables that determine structural performance, *e.g.*, flow strength, fracture toughness, applied stress and flaw size. Failure is predicted for all combinations of these variables satisfying $g(X_i) \le 0$, so the assessment calculations seek to determine the fraction of their joint probability density falling outside the limit state. This fraction represents the probability of failure (P_f).

The two failure modes typically considered in the assessment of flawed girth welds are unstable fracture and plastic collapse. The Level 2 Failure Assessment Diagram (FAD) method of BS 7910 [5] (formerly PD 6493) combines both of these into a single graphical format, which had been the basis of the owner/operator's previous acceptance criteria. However, experience has shown that limit state functions based on FAD expressions are often problematic for the algorithms employed by probabilistic analysis codes. These problems are generally not intractable, but can be time-consuming to debug. Under the time and budget constraints of this project, it was decided that the probabilities of fracture and collapse would be calculated separately.

Fracture. Using the fracture assessment parameter K_r given by BS 7910, formulated in terms of crack-tip opening displacement (CTOD), evaluations of the probability of failure due to unstable fracture were based on an expanded version of the expression:

$$P_f^{Frac} = P\left[1 - \left(\sqrt{\frac{\delta_e^{App} + \delta_e^{Q}}{\delta_{mat}}} + \rho\right) \le 0\right] \tag{2}$$

The driving force for fracture was defined as the elastic component of the applied CTOD, denoted as δ_e^{App} and δ_e^{Q} for the respective contributions of the applied (seismic) and residual stresses. δ_{mat} represents the measured fracture resistance (critical CTOD) of the girth weld metal, and ρ is a plasticity correction factor.

It has been shown [4] that secondary bending induced by a bell geometry essentially the same as that of the BBCR joints in the subject pipeline has negligible effect on the stress intensity (or applied CTOD) associated with a girth weld flaw. A stress intensity solution developed by Wang *et. al* [6] for flaws of finite length in straight joints was therefore adopted as the basis for crack driving force due to applied (seismic) stresses:

$$K_I^{App} = S_{Seis}\sqrt{\pi a}F_b$$

$$\text{where: } F_b = \left[-0.07039 + \frac{\beta}{\alpha}\left(m_1 + m_2\left(\frac{\beta}{\alpha}\right)^{-0.5565} + m_3\left(\frac{\beta}{\alpha}\right)\right)\right]$$

$$\text{for } \frac{D}{t}\cdot\beta \le \frac{32}{\pi}\cdot\eta \tag{3}$$

and where:

$$\alpha = \left(\frac{42}{D/t}\right)^{1.2}$$

$$m_1 = -2392.1\eta^4 + 5243.9\eta^3 - 4169.2\eta^2 + 1476.0\eta - 214.05$$

$$m_2 = 5.4791\eta^{-0.4654}$$

$$m_3 = \exp\left(10.500\eta^2 - 18.171\eta + 8.6538\right)$$

and where:

$$F_b = F_b \quad \text{at} \quad \frac{32}{\pi}\frac{\eta}{D/t} \quad \text{for} \quad \frac{D}{t}\cdot\beta > \frac{32}{\pi}\cdot\eta$$

S_{Seis} is the applied seismic stress, a is the flaw height, parameter η is flaw height expressed as a fraction of pipe wall thickness (t = 0.3125 in.), and parameter β is flaw length expressed as a fraction of pipe circumference (πD, where D = 22 in.).

In addition to externally-applied stresses, welding-induced residual stresses can also contribute to the unstable fracture driving force. Girth weld residual stresses in large D/t pipes are governed primarily by an axisymmetric bending moment induced by shrinkage in the hoop direction, causing tension at the root and compression at the cap. According to Michaleris *et al* [7], the total stress intensity due to weld residual stresses acting on a circumferential, internal surface crack (K_I^Q) is best estimated by combining the solution of Gordon, *et al* [8] with the series solution of Buchalet [9], giving:

$$K_I^Q = S_Q\sqrt{\pi a}\left[1.1 + A\left(6\eta^b + \eta^c\right)\right] - S_Q\sqrt{\pi a}\left[0.6657\eta + 0.02646\eta^2 + 0.9368\eta^3\right]$$

$$\text{where: } A = -0.6259 + 0.5207\left(\frac{D}{t}\right)^{0.2} \tag{4}$$

$$b = 1.544 + \left(2.414\times10^{-2}\right)\left(\frac{D}{t} - 20\right)^{0.6}$$

$$c = 2.649 + 0.6959\left(\frac{D}{t} - 20\right)^{0.25}$$

and where S_Q is the maximum (root surface) tension value. The first (Gordon) half of the equation establishes the stress intensity the crack tip would experience if the root surface tension value existed over the full wall thickness. The second (Buchalet) half effectively reduces this value to account for the through-thickness stress gradient that is actually present.

The use of Equations (3) and (4) with CTOD as the definition of crack driving force due to applied and residual stresses (δ_e^{App} and δ_e^{Q}) required a conversion from K_I, which in the present case was:

$$\delta_e = d_n\frac{J_e}{S_Y}$$

$$\text{where: } d_n = 4.3238\left(\frac{1}{n}\right)^2 - 3.1122\left(\frac{1}{n}\right) + 0.7868 \tag{5}$$

$$\text{and: } J_e = \frac{K_I^2}{E/\left(1-\nu^2\right)}$$

where J_e is the elastic component of the plane-strain *J*-integral value, S_Y is the material yield strength, *n* is the strain hardening exponent, *E* is the modulus of elasticity and ν is Poisson's ratio [6,10].

Plastic Collapse. Evaluations of the probability of failure due to plastic collapse were based on an expanded version of the expression:

$$P_f^{Coll} = P\left[S_C - S_{Seis} \le 0\right] \tag{6}$$

Computational and experimental work reported by Wang *et al* [6,10] has shown the Miller solution to be the most accurate of the several available for girth weld plastic collapse prediction. However, experience has again shown that the cyclic (sine and cosine) functions in the Miller solution tend to be problematic for the algorithms employed by probabilistic analysis codes. The second most accurate (only 7% less so, and in the conservative direction), is one given by Wilkowski and Eiber [11]. It was adopted as the basis for plastic collapse assessment:

$$S_C = S_F\left[\frac{1-\eta}{1-\frac{\eta}{N}}\right] \tag{7}$$

$$\text{where: } N = \sqrt{1+0.26\beta+47\beta^2-59\beta^3}$$

and where S_F is the flow strength, typically defined as the average of yield and ultimate tensile.

Characterizing Input Parameters

As dictated by the two limit state functions defined above, the input parameters adopted as random variables for the probabilistic assessment were:

- Relative flaw height and length (η and β)
- Applied (seismic) stresses (S_{Seis})
- Residual stresses (S_Q)
- Fracture resistance in terms of critical CTOD (δ_{mat})
- Weld metal flow strength (S_F)

Deterministic (singular), conservative values were adopted for a number of other variables:

- Modulus of elasticity
- Poisson's ratio
- Yield strength (only for K_I to δ_e conversion)
- Strain hardening exponent
- ρ (plasticity correction factor)
- Pipe diameter and wall thickness

In preparation for this assessment, the owner/operator had contracted with a reputable laboratory to conduct a fairly comprehensive characterization of four girth welds taken from straight joints in the subject pipeline, three of them BBCR and one having a chill ring without belled pipe ends. Their evaluation included macro-examination of weld cross-sections, hardness tests, residual stress measurements, analyses of chemical composition, cross-weld tensile strength of both standard and wide-plate specimens, additional breakage of specimens to reveal weld flaw geometries, and fracture toughness tests [12].

Following are descriptions of the work undertaken to characterize and incorporate these and other available data into the assessment framework.

Flaw Dimensions. Nondestructively-measured height and length data from 284 BBCR girth weld flaws found in the subject pipeline were provided to this project by the owner/operator. To simplify the limit state function for the fracture assessment, as well as to ensure that in terms of δ_e^{App} and δ_e^{Q} the *combined* effects of height and length of each flaw were accurately represented, two new random variables F_{App} and F_Q were created, as:

$$F_{App} = \sqrt{a}F_b$$

and (8)

$$F_Q = \sqrt{a}\left[\left(1.1+A\left[6\eta^b+\eta^c\right]\right)-\left(0.6657\eta+0.02646\eta^2+0.9368\eta^3\right)\right]$$

Values of F_{App} and F_Q were computed for each flaw, then their maximum values were extracted from each girth weld. Unstable fracture is a 'weakest link' failure mode, in that the single flaw representing the largest value of δ_e determines the nominal stress for fracture initiation. The resulting data were then processed and examined to determine their mean values (μ), standard deviations (σ) and distribution types, using a combination of statistical tests (method of moments, Kolmogorov-Smirnov and Chi-square), prior firsthand experience [*e.g.*, 4,13], knowledge of other investigators' findings [*e.g.*, 14], and engineering judgment. Figures 1 and 2 show the probability density functions (PDF) and cumulative distribution functions (CDF) that were established for F_{App} and F_Q. Both were modeled as Type I Extreme Value (EVD I), which represents distributions of maxima.

The correlation coefficient between F_{App} and F_Q indicated a rather high value of 0.82, not surprising given that both parameters are strongly dependent on flaw height, and especially since most of their respective maxima were due to the very same flaw. This effect was included in the probabilistic analysis.

A comparison of flaw heights made visible on fracture surfaces by the wide plate tests with those measured ultrasonically by the owner/operator indicated generally close agreement, within 0.01 inch in all but one case. In that particular case, the exposed flaw was 0.04 inch taller than any of the measured values for that weld. Similar comparisons between other fracture surfaces produced intentionally for the purpose of comparison with ultrasonic data showed close agreement.

For the plastic collapse assessment, flaw height and length were again combined into a single random variable, this time as the strength reduction factor enclosed in square brackets in Equation (7). However, since the distribution of that quantity was of a nonstandard shape and found to be problematic, its inverse was instead defined as a new parameter F_{Coll} for purposes of distribution fitting:

$$F_{Coll} = \left[\frac{1-\eta}{1-\frac{\eta}{N}}\right]^{-1} \tag{9}$$

with the plastic collapse limit state modified accordingly as:

$$P_f^{Coll} = P\left[\frac{S_F}{F_{Coll}} - S_{Seis} \le 0\right] \tag{10}$$

Values of β for calculating values of F_{Coll} were based on the *total* flaw length for each weld, accompanied by a length-weighted average flaw height, calculated as:

$$\eta_{avg} = \sum_{i=1}^{n} \eta_i \left(\frac{\beta_i}{\beta_{tot}} \right) \tag{11}$$

where *n* is the total number of flaws found in a given weld.

The resulting values of F_{Coll} were processed and examined to determine mean (μ), standard deviation (σ) and distribution type, again using a combination of statistical tests and engineering judgment. Figure 3 shows the PDF and CDF that were established. As with F_{App} and F_Q, it was found that F_{Coll} was best modeled as a Type I EVD.

Applied (Seismic) Stresses. Using PIPLIN [15], a computational deformation analysis was performed on each of the five pipeline segments. A series of ground movement profile sequences was applied to each segment, with each sequence representing one combination from a matrix of various soil displacement amplitudes and three different along-the-ground-contour 'block' profile widths. Each displacement profile was traversed across each segment in 100-ft. position increments to comprise each sequence (Figure 4). Eight to thirteen different displacement amplitudes were applied in this manner, with the upper-bound amplitude for each segment based on guidelines provided by the owner/operator's geotechnical staff. The results provided various demand effects (axial force, bending moment, maximum axial tension and compression stresses) at the node corresponding to the maximum pipeline curvature location for each position of the profile.

It was most convenient from the standpoint of the form of both limit state functions, as well as most relevant to the failure modes of interest, to use tensile stress as the input parameter. Since it was not computationally feasible to record and store the peak stress at each weld location, it was decided to extract the largest value from each series of profile positions, and assume that any weld within the region could experience that value.

Instructions given by the owner/operator's geotechnical staff were to assess P_f separately for each of the three different profile widths (100, 550 and 1000 feet), without attempting to rank their relative probabilities. Based on further discussions, a simple but reasonable distribution-fitting approach was formulated for the range of maximum applied tensile stresses predicted by PIPLIN for each permutation of segment and profile width. The mean value was calculated in the usual way, then the applied stress resulting from the upper-bound soil displacement was assigned a cumulative probability of 0.99. Assuming a normal (Gaussian) distribution, fixing the mean and 99th percentile values determined the standard deviation. Fifteen different distributions were thus identified, of which two representative examples are given in Figures 5 and 6.

Given the highly stochastic nature of seismic ground motion, demand effects are perhaps the most uncertain of all relevant assessment inputs. It should therefore be noted that all of the estimated displacements and profile widths were based on a single, 10% in 50-year (500-year return period) postulated seismic event. As such, this assessment did not address the full spectrum of possible events and their associated likelihoods. It was essentially an assessment of a single 'design case' event with all of its possible pipeline demand outcomes, in terms of their probability of producing one or more girth weld failures.

It should also be noted that the much smaller stresses induced by the Poisson effect were justifiably omitted, since the overall peak stresses would occur at a moment when pipe and soil were essentially decoupled.

Residual Stresses. It has been shown that in large (>~40) *D/t* pipes, the magnitude of the tensile residual stress at the root of a girth weld is approximately equal to that of the compressive value measured on the weld cap surface at the same circumferential position [7]. Measurements of this kind had been performed by the aforementioned laboratory using the blind hole drilling (BHD) method at four locations, 90 degrees apart, on each of the four girth welds removed from the pipeline (Figure 7) [12]. Their data indicated at least one location in each weld where the sign of the through-thickness residual stress profile was reversed; these values were conservatively omitted. The remaining 12 data were processed to obtain the normal distribution of S_Q shown in Figure 8.

It should be noted that while residual stresses can play a significant role in the initiation of unstable fracture, they generally do not contribute to plastic collapse events. In the present assessment they were treated as such.

Fracture Resistance (CTOD). The laboratory conducted tests on 16 specimens taken from the four welds to provide CTOD data for fracture assessment [12]. Elevated loading rates such as those resulting from seismic events typically increase the ductile-to-brittle transition temperature (DBTT) for structural steels. The temperature shift recommended by Barsom [16] was employed to account for this, and the resulting test temperatures ranged from 14 to 19°F. Even at these low temperatures, all but one of the specimens exhibited limit load behavior. The resulting data were processed to obtain the Weibull distribution of δ_{mat} shown in Figure 9.

Flow Strength. Also performed were 16 cross-weld tensile tests to provide yield and ultimate tensile strength data. Flow strength (S_F), the resistance variable in the plastic collapse assessment, was conservatively defined as the stress midway between yield and ultimate tensile. The resulting data, most of which were corrected to account for the presence of flaws, were processed to obtain the normal distribution of S_F shown in Figure 10.

Miscellaneous Constants. As mentioned previously, several input parameters were applied deterministically, *i.e.*, as single values. Table 1 summarizes these, most of which were used only to convert crack driving force from K_I to δ_e. The assumed value of yield strength (S_Y) was two standard deviations below the mean value ($\mu - 2\sigma$) of the available data. The use of deterministic variables for ρ, *D* and *t* was motivated primarily by time and budget constraints, although typical variations in *D* and *t* have been shown to have negligible influence on P_f for both of the limit states being considered [13].

TABLE 1. Deterministic Input Values

Constant	Value	Purpose
Modulus of elasticity (*E*)	30,000 ksi	K_I to δ_e conversion
Poisson's ratio (ν)	0.3	K_I to δ_e conversion
Yield strength (S_Y)	36 ksi	K_I to δ_e conversion
Strain hardening exponent (*n*)	8.5	K_I to δ_e conversion
Plasticity correction factor (ρ)	0.066	P_f^{Frac} calculation
Pipe diameter (*D*)	22 in.	β calculation
Pipe wall thickness (*t*)	0.3125 in.	η calculation

Calculating Failure Probabilities

Using Equations (2) and (10) and the various probabilistic and deterministic parameters given above, calculations of P_f for both fracture and plastic collapse were performed using the Monte Carlo Simulation (MCS) algorithm in NESSUS® [17]. To ensure adequate accuracy for the P_f values that were computed for each failure mode, 3.5 million MCS trials were conducted for each fracture case, and 100,000 for each plastic collapse case. 95% confidence intervals due to MCS sampling error indicated maximum possible errors ranging from ±16.5% to ±54.5% for the various fracture cases. Due to the significantly higher values of P_f^{Coll}, 95% confidence intervals on computed collapse probabilities ranged from ±1.8% to ±29.2%. For both failure modes, and as was expected, the largest confidence intervals were associated with the smallest values of P_f.

To estimate the total failure probability of each segment for both fracture and collapse, the pipeline was treated as a system of elements (girth welds) in series. If failures of the individual elements in a series system are perfectly correlated to one another, P_f for the system can be defined simply as:

$$P_{f_{Sys}} = \max_i \left(P_{f_i} \right) \tag{12}$$

where P_{f_i} is the failure probability of any single weld in the segment of interest. Since all of the girth welds in each segment were assumed to have the same chance of failure, Equation (12) reverted to $P_{f_{Sys}} = P_f$ as defined by Equations (2) or (10). If individual failures are statistically independent from one another (*i.e.*, perfectly *un*correlated), P_f for the system can be defined as:

$$P_{f_{Sys}} = 1 - \prod_{i=1}^{n} \left(1 - P_{f_i} \right) \tag{13}$$

where n is the total number of girth welds in any segment of interest. Again, since all girth welds within each segment were assumed to have an equal chance of failure, Equation (13) reverted to:

$$P_{f_{Sys}} = 1 - \left(1 - P_{f_i} \right)^n \tag{14}$$

First-order bounds were thereby placed on the girth weld reliability for each segment. Some degree of failure correlation among the girth welds throughout the line can be expected, since a particular seismic event may apply similar stresses to all of them. On the other hand, the material properties and flaw sizes fluctuate more or less randomly from one weld to another. The actual girth weld P_f for the system (pipeline segment) can be taken to lie somewhere between these two extremes.

Calculations based on Equation (14) assumed that girth welds occur at 30-ft. intervals over the entire length of each segment. For both fracture and plastic collapse, Table 2 provides lower- and upper-bound values of P_f for the segment associated with each segment and ground movement profile width.

DISCUSSION

In evaluating the various failure probabilities given in Table 2, the reader is reminded that they were based on a postulated 'design case' seismic event having a 10% in 50-year probability of occurrence (500-year return period). Their overall likelihoods are therefore far less than those shown. Bearing that reality in mind, two general conclusions can be drawn: first, that unstable fracture is highly unlikely, regardless of model region or ground motion profile width, and second, that plastic collapse is likely to occur in several cases. This was essentially inevitable, given the range of applied stresses predicted for those cases, and has less to do with flaw sizes than with the sheer magnitude of the stresses. Nonetheless, the lack of appreciable weld metal strength overmatching in older pipelines [4,12] does contribute to this problem, since it precludes the usual assumption that plastic strain will distribute more or less uniformly across the joint, rather than localize at flaws in the weld metal.

However, the latter is not necessarily a reason for grave concern, since plastic collapse indicates imminent failure only in load- or stress-controlled, not strain- or displacement-controlled events. Much like the onset of necking in a standard uniaxial tensile test specimen, which defines the engineering property known as ultimate tensile strength, plastic collapse indicates the far-field (nominal) stress at which the load-carrying capacity of a girth weld begins to decline. It does *not* define the strain level at which separation occurs. When assessing the structural fitness of a pipeline that may experience significant ground movement, strain (rather than load) capacity is typically the relevant parameter, since a pipeline is generally not required to resist such motion, merely to accommodate it. All but one of the cross-weld wide plate test results from samples containing flaws at the upper end of the size range found in this pipeline indicated crosshead displacements of 0.25 to over 0.42 in. prior to separation [12]. The lone exception contained an unusually large flaw. Before identifying the present P_f^{Coll} results as problematic, it would be useful to revisit the PIPLIN model output to determine whether per-unit-length displacements of similar magnitude would be expected in the most severe cases.

The owner/operator did not make the necessary FFS decisions for each segment solely on the basis of the results presented here. These were incorporated into a system-wide risk management and GIS program for allocating maintenance resources according to various potential causes and consequences of failure. As such, it is not possible to identify which of the P_f values given in Table 1 were considered acceptable and which were not. It must suffice to say that no immediate action was required.

Finally, it should also be noted that the results presented here are specific to a particular (and fairly unusual) pipeline operating under a specific set of conditions, thus have very limited applicabilty to other situations. However, the assessment methodology can be adapted and applied to most situations.

CONCLUSIONS AND RECOMMENDATIONS

1. Given the occurrence of a 500-year seismic event, the predicted maximum probability of girth weld unstable fracture within any particular segment was less than 0.1% in over half of the cases evaluated, and less than 1% in all cases.
2. Also given the occurrence of a 500-year seismic event, the predicted maximum probability of girth weld plastic collapse within any particular segment was moderately to very high in several cases. However, this was not necessarily cause for immediate action, since pipeline loading is essentially strain- or displacement-controlled, which lessens the relevance of plastic collapse as a limit state.
3. The PIPLIN analysis results should be revisited to compare predicted axial strain levels to the maximum per-unit-length crosshead displacements measured in cross-weld wide-plate tests.

4. Seismic events representing various other return periods should be modeled in order to construct a complete hazard curve for each segment. This would enable the full spectrum of event likelihood to be incorporated into calculations of failure probability for these and other limit states, thus providing a more realistic assessment of seismic fitness.

ACKNOWLEDGEMENTS

This work was performed under Gas Research Institute Contract 800701.003, and the helpful oversight of GRI program manager Mr. Chuck French is gratefully acknowledged. It could not have been completed without the invaluable guidance of the owner/operator's pipeline engineering and geotechnical staff. The timely assistance of Mr. David Riha of Southwest Research Institute was also most appreciated.

REFERENCES

[1] Litehiser, J. J., Abrahamson, N. A. and Arango, I., "Wave-Induced Axial Strain of Buried Pipes," Columbian Geotechnical Society, date unknown.

[2] Newmark, N. M., "Problems in Wave Propagation in Soil and Rock," *Proceedings of the International Symposium on Wave Propagation and Dynamic Properties of Earth Materials*, August 23-25, University of New Mexico Press, pp. 7-26.

[3] Honegger, D. G. and Nyman, D. J., *Guidelines for the Seismic Design and Assessment of Natural Gas and Liquid Hydrocarbon Pipelines*, Final Report, PRCI Contract PR-268-9823, PRC International, October 2004.

[4] Warke, R. W., Koppenhoefer, K. C. and Amend, W. E., "Seismic Fitness of Girth Welds in an Early-1930s Vintage Gas Transmission Line," Proceedings of the 1997 *Pipeline Risk Management & Reliability Conference*, Houston, 1997, Clarion Technical Conferences and Scientific Surveys Ltd.

[5] BS 7910:1999, *Guide on Methods for Assessing the Acceptability of Flaws in Metallic Structures*, British Standards Institution, 1999.

[6] Wang Y.-Y., Rudland, D., and Horsley, D., "Development of a FAD-Based Girth Weld ECA Procedure: Part I – Theoretical Framework," Paper IPC2002-27171, *Proceedings of the 4th International Pipeline Conference*, Calgary, Alberta, Canada, Sep. 29–Oct. 3, 2002.

[7] Michaleris, P., Kirk, M. T. and Laverty, K., *Incorporation of Residual Stresses into Fracture Assessment Models*, Final Report, EWI Project 01236IRP, December 1996.

[8] Gordon, J. R., Wang, Y-Y. and Dong, P., "The Development of Fitness-for-Purpose Flaw Acceptance Criteria for Sleeve Connections," *8th Symposium on Line Pipe Research*, PRC International, September 1993.

[9] Buchalet, C. B. and Bamford, W. H., "Stress Intensity Factor Solutions for Continuous Surface Flaws in Reactor Pressure Vessels," in *Mechanics of Crack Growth*, ASTM STP 590, pp. 385-402, ASTM, 1976.

[10] Wang Y.-Y., Rudland, D., and Horsley, D., "Development of a FAD-Based Girth Weld ECA Procedure: Part II – Experimental Verification," Paper IPC2002-27173, *Proceedings of the 4th International Pipeline Conference*, Calgary, Alberta, Canada, Sep. 29–Oct. 3, 2002.

[11] Wilkowski, G. M. and Eiber, R. J., "Evaluation of Tensile Failure of Girth Weld Repair Grooves in Pipe Subjected to Offshore Laying Stresses," *J. Energy Resources Technology*, vol. 103, pp. 48-55, 1981.

[12] Orth, F., *Material Properties of […] Gas Transmission Line No. […] Girth Weld Samples*, Final Report, EWI Project 43982CAP, August 2003.

[13] Warke, R. W. and Ferregut, C. M., "Reliability-Based Fitness-for-Service Assessment of Pipeline Girth Welds," Final Report, PRCI Contract PR-185-9429, PRC International, August 1998.

[14] Gianetto, J. A., Shen, G., Tyson, W. R., and Glover, A. G., "Assessment of the Fracture Toughness of Pipeline Girth Welds," *Proceedings of the 5th International Conference on Trends in Welding Research*, pp. 916-921, ASM International, 1998.

[15] SSD, Inc., PIPLIN: *Computer Program for Stress and Deformation Analysis of Pipelines*, Version 4.54, User Reference and Theoretical Manual, Reno, Nevada, March 2006.

[16] Barsom, J. M., "Effect of Temperature and Rate of Loading on the Fracture Behaviour of Various Steels," Paper 31 in *Dynamic Fracture Toughness: Proceedings of the International Conference*, July 1976, pp. 113-125, The Welding Institute, 1977.

[17] Riha, D. S, Thacker, B. H., Enright, M. P., Huyse, L. and Fitch, S. H. K., "Recent Advances of the NESSUS Probabilistic Analysis Software for Engineering Applications," *Proceedings 42nd AIAA/ASME/ASCE/AHS/ASC Structures, Structural Dynamics, and Materials (SDM) Conference*, AIAA-2002-1268, Denver, Colorado, April 2002.

TABLE 2. Predicted Probabilities of Fracture and Plastic Collapse

Segment	Stress Input and Result Type		Profile Width (ft.)		
			100	550	1000
1	S_{Seis} (ksi)	μ	36.35	38.03	36.65
		σ	2.38	2.26	1.69
	Segment P_f^{Frac}	Min.	4.9×10^{-6}	6.0×10^{-6}	5.7×10^{-6}
		Max.	9.2×10^{-4}	1.1×10^{-3}	1.1×10^{-3}
	Segment P_f^{Coll}	Min.	1.1×10^{-3}	2.1×10^{-3}	8.5×10^{-4}
		Max.	0.18	0.32	0.15
2	S_{Seis} (ksi)	μ	36.39	46.46	45.43
		σ	0.99	3.88	3.72
	Segment P_f^{Frac}	Min.	5.1×10^{-6}	3.3×10^{-5}	2.8×10^{-5}
		Max.	1.2×10^{-3}	7.6×10^{-3}	6.5×10^{-3}
	Segment P_f^{Coll}	Min.	4.9×10^{-4}	7.9×10^{-2}	5.8×10^{-2}
		Max.	0.11	~1.0	~1.0
3	S_{Seis} (ksi)	μ	35.12	36.42	36.53
		σ	3.26	4.25	4.20
	Segment P_f^{Frac}	Min.	3.7×10^{-6}	4.9×10^{-6}	4.9×10^{-6}
		Max.	3.4×10^{-4}	4.5×10^{-4}	4.5×10^{-4}
	Segment P_f^{Coll}	Min.	9.6×10^{-4}	3.2×10^{-3}	3.3×10^{-3}
		Max.	0.09	0.26	0.27
4	S_{Seis} (ksi)	μ	35.68	36.28	36.31
		σ	1.68	1.55	1.54
	Segment P_f^{Frac}	Min.	4.6×10^{-6}	5.1×10^{-6}	5.1×10^{-6}
		Max.	4.5×10^{-4}	5.0×10^{-4}	5.0×10^{-4}
	Segment P_f^{Coll}	Min.	4.5×10^{-4}	5.9×10^{-4}	5.9×10^{-4}
		Max.	0.04	0.06	0.06
5	S_{Seis} (ksi)	μ	37.01	47.78	43.40
		σ	0.98	3.79	2.79
	Segment P_f^{Frac}	Min.	6.0×10^{-6}	4.0×10^{-5}	1.9×10^{-5}
		Max.	4.3×10^{-4}	2.9×10^{-3}	1.3×10^{-3}
	Segment P_f^{Coll}	Min.	7.2×10^{-4}	0.11	2.5×10^{-2}
		Max.	0.05	~1.0	0.84

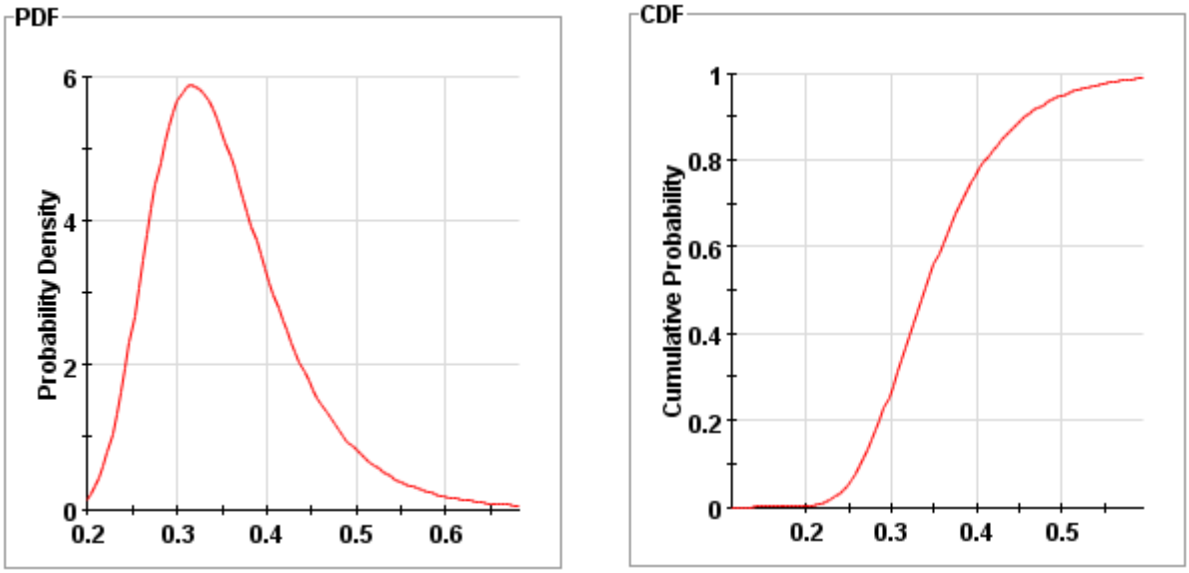

FIGURE 1. PDF and CDF of parameter F_{App} ($\mu = 0.353$; $\sigma = 0.0804$)

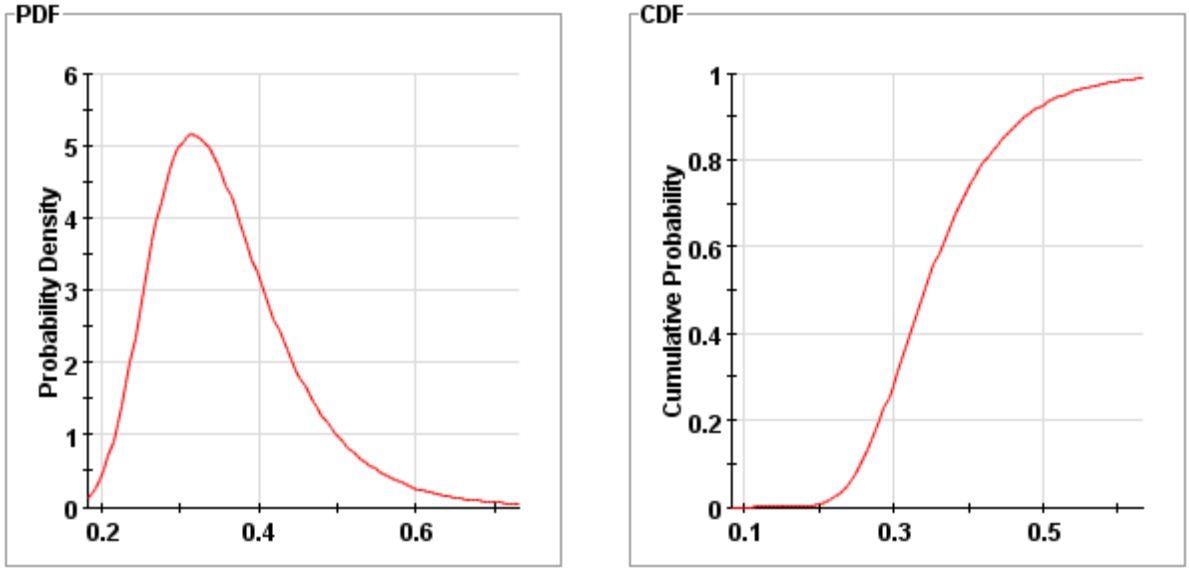

FIGURE 2. PDF and CDF of parameter F_Q ($\mu = 0.357$; $\sigma = 0.0917$)

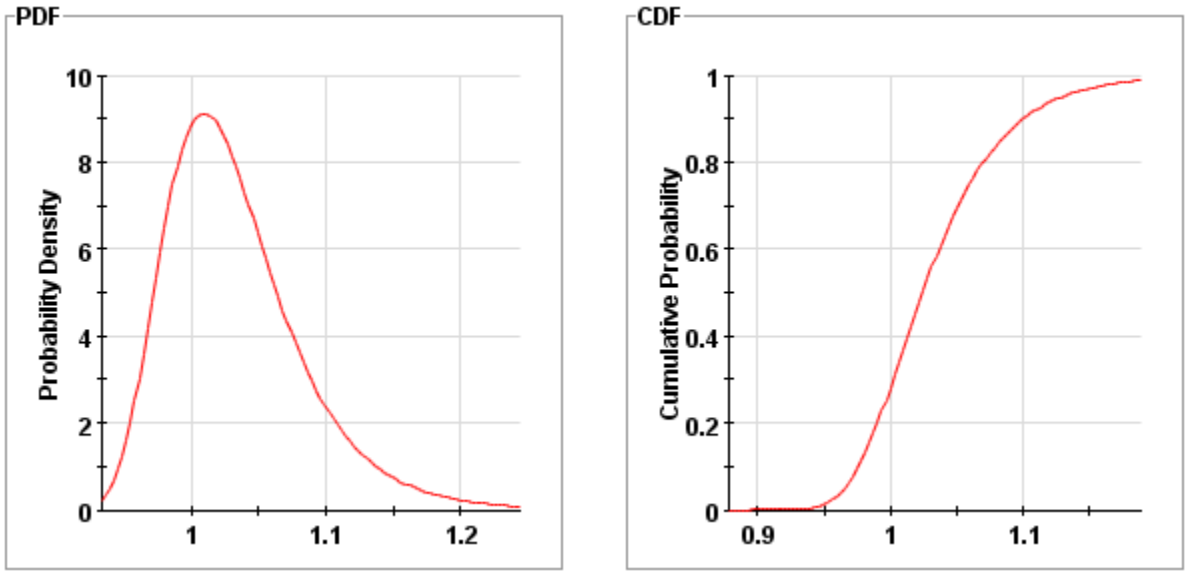

FIGURE 3. PDF and CDF of parameter F_{Coll} (μ = 1.0327; σ = 0.0517)

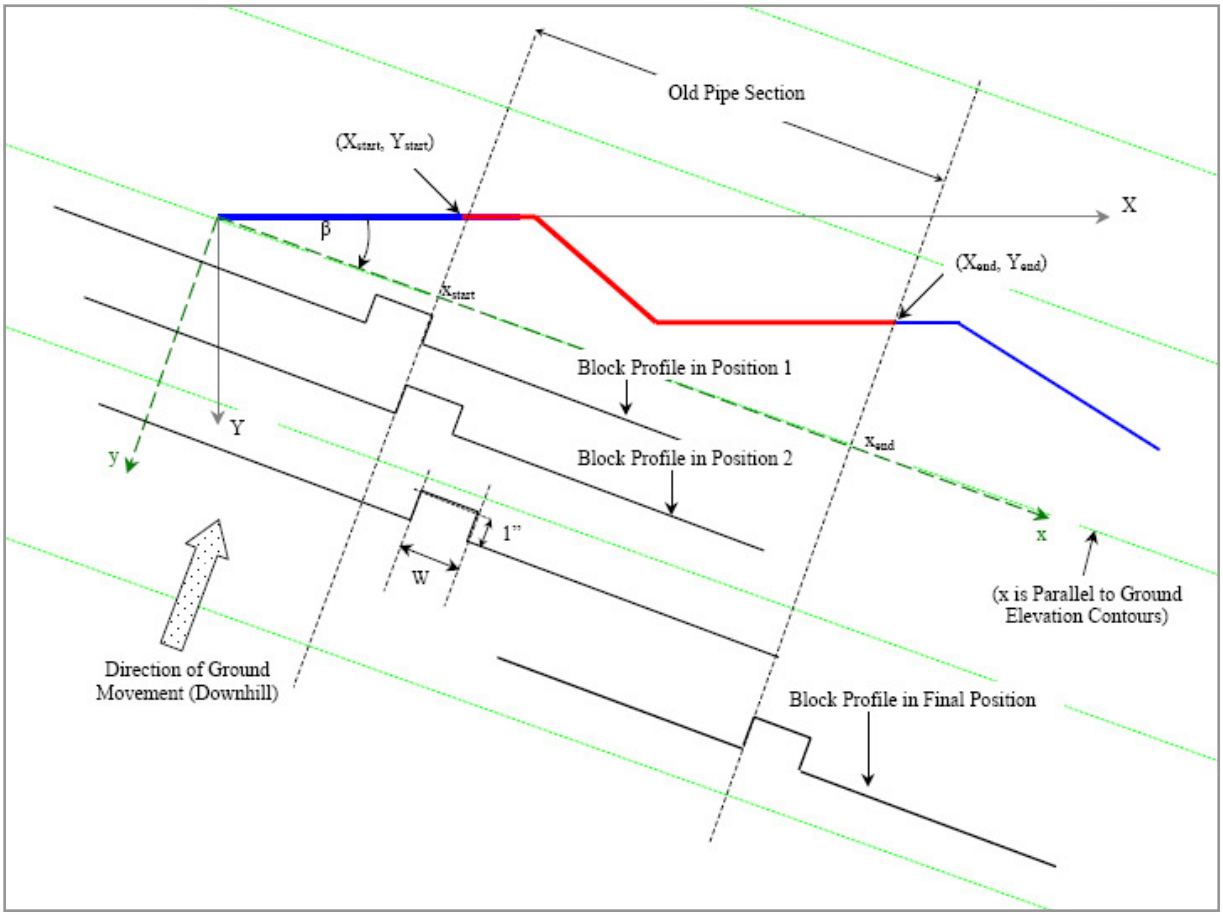

FIGURE 4. Example of Ground Movement Profile Application to Pipeline Segment

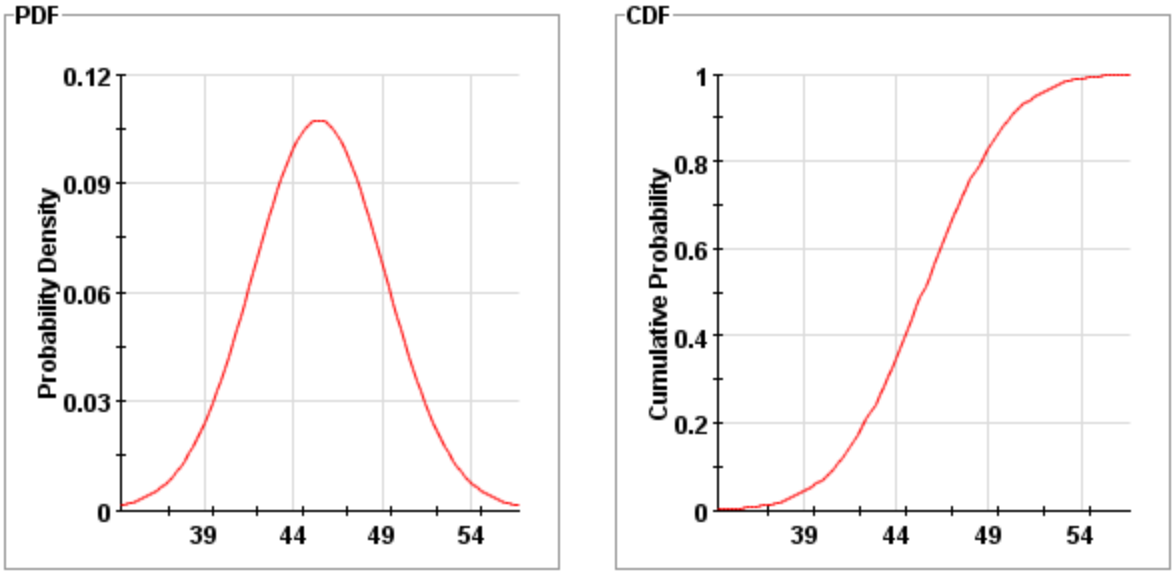

FIGURE 5. PDF and CDF of parameter S_{Seis} for Segment 2 with a profile width of 1000 ft. (μ = 45.43 ksi; σ = 3.72 ksi)

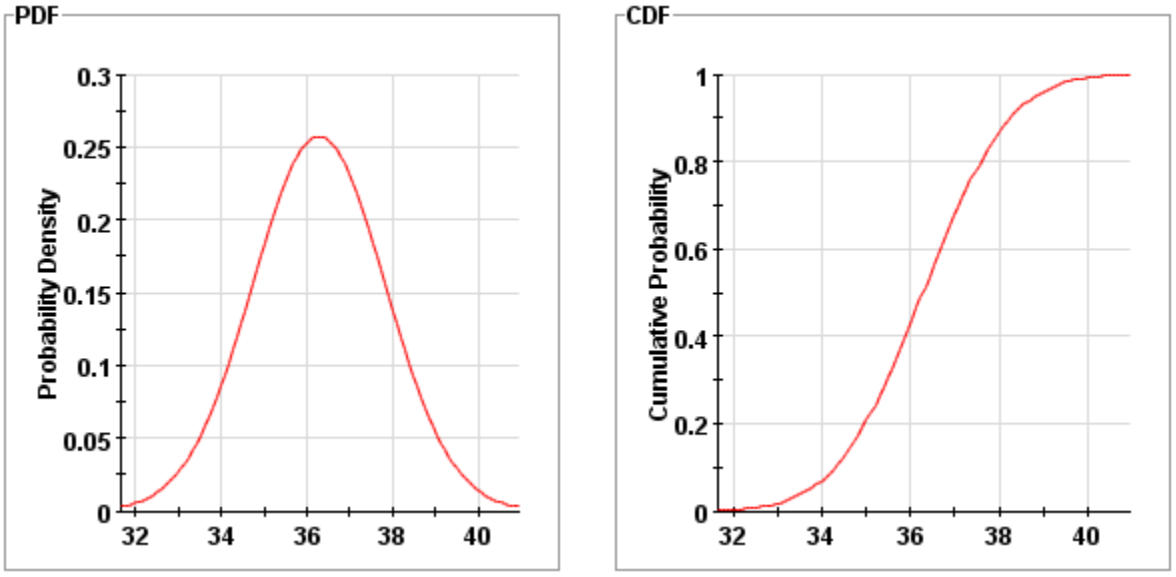

FIGURE 6. PDF and CDF of parameter S_{Seis} for Segment 4 with a profile width of 550 ft. (μ = 36.28 ksi; σ = 1.55 ksi)

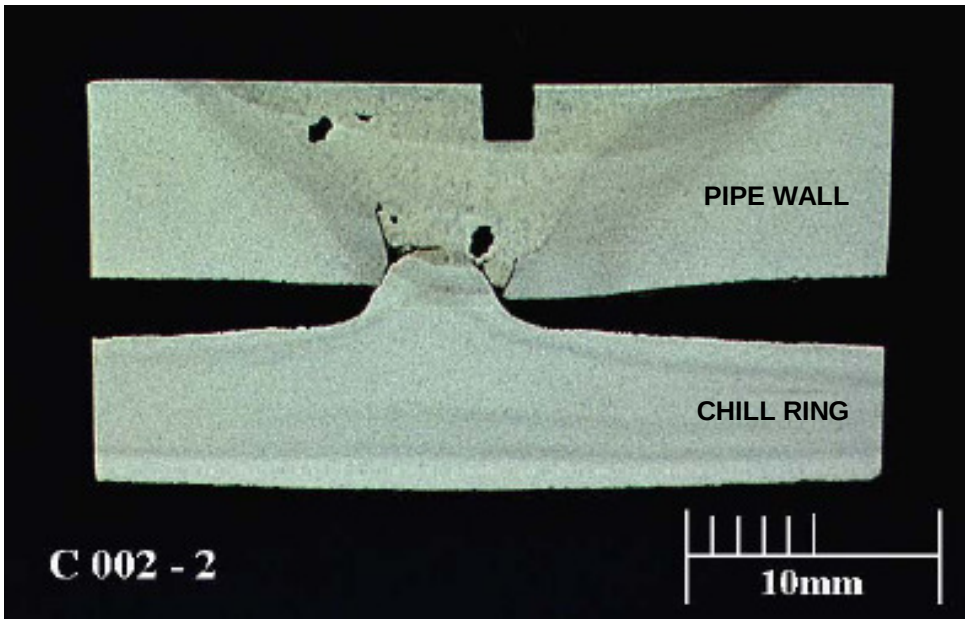

FIGURE 7. Example of Section through Girth Weld Showing Location of BHD Residual Stress Measurement

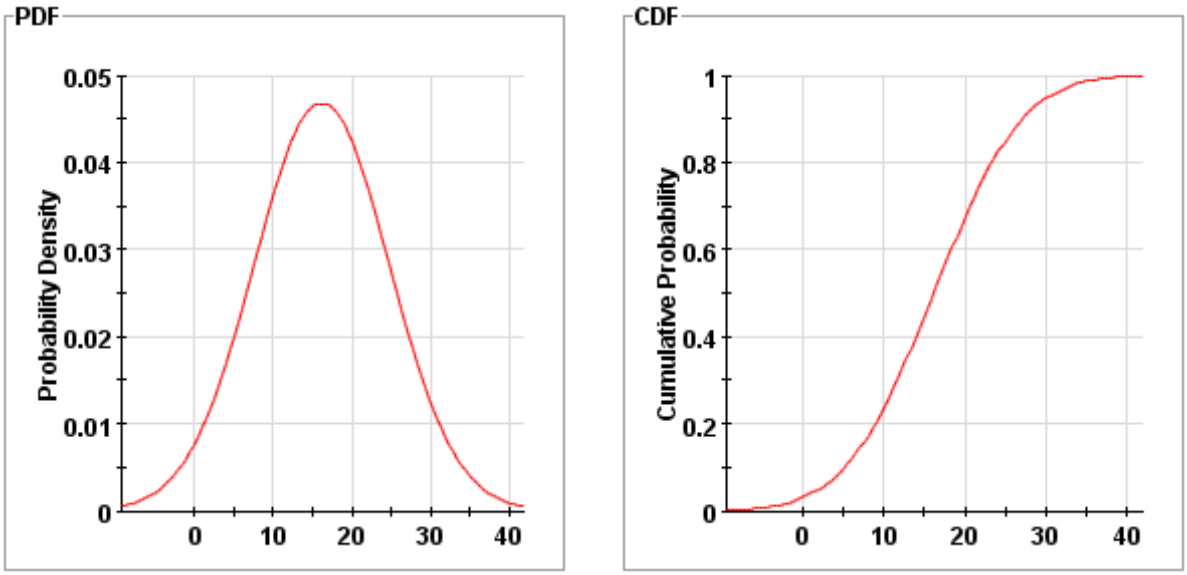

FIGURE 8. PDF and CDF of parameter S_Q (μ = 16.16 ksi; σ = 8.53 ksi)

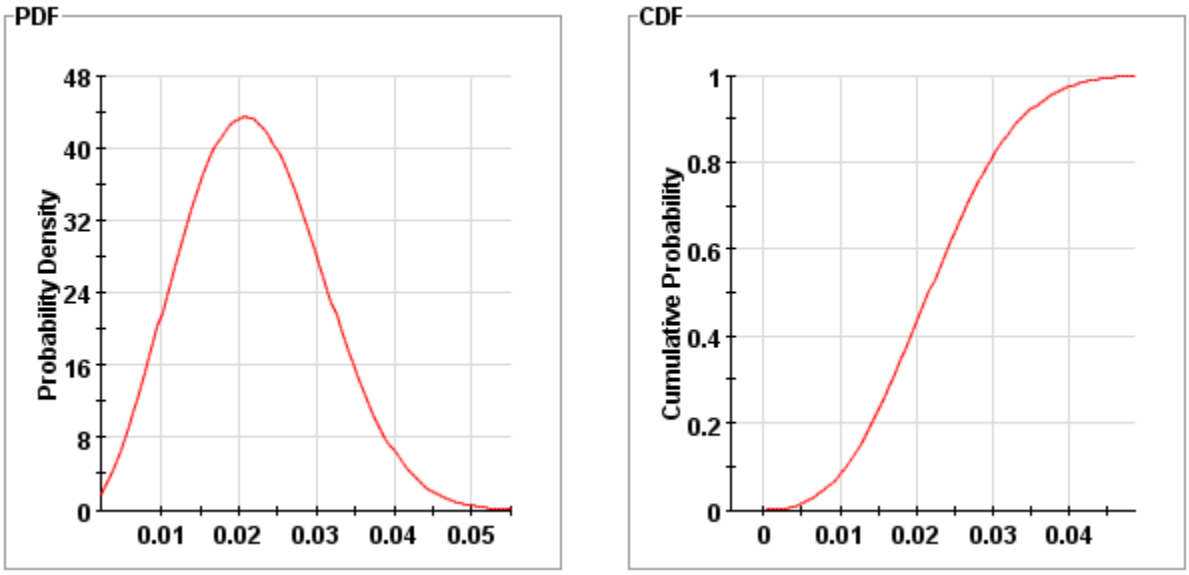

FIGURE 9. PDF and CDF of parameter δ_{mat} (μ = 0.022 in.; σ = 0.0088 in.)

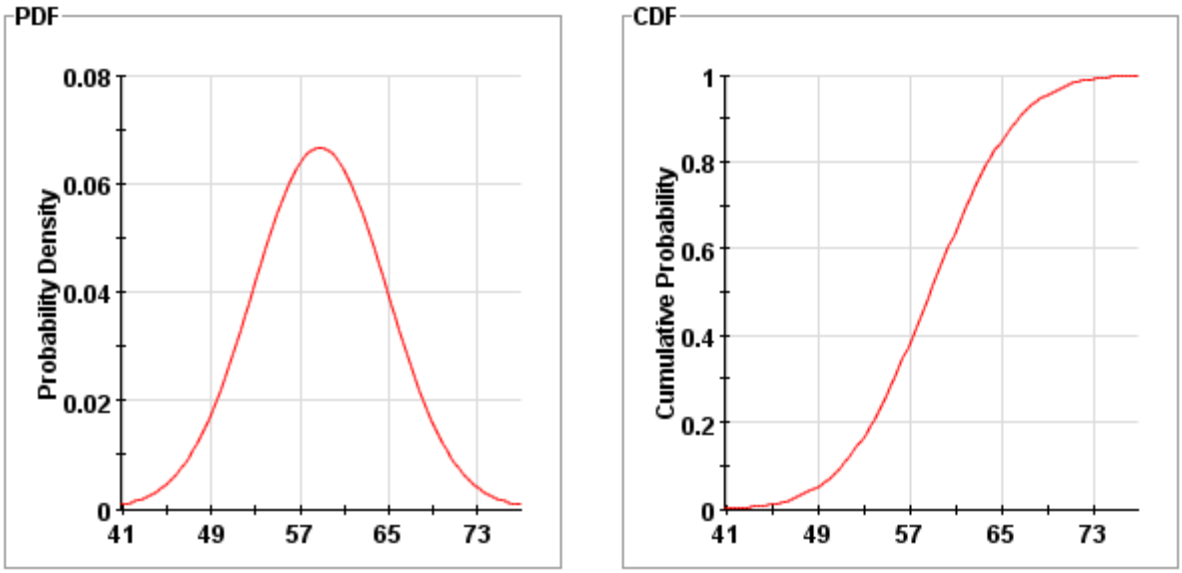

FIGURE 10. PDF and CDF of parameter S_F (μ = 58.8 ksi; σ = 6.0 ksi)